Adjoint-based Optimization Procedure for Active Vibration Control of Nonlinear Mechanical Systems

Carmine M. Pappalardo
Research Fellow
Department of Industrial Engineering
University of Salerno
Via Giovanni Paolo II
132, 84084 Fisciano, Salerno, Italy
Email: cpappalardo@unisa.it

Domenico Guida
Professor
Department of Industrial Engineering
University of Salerno
Via Giovanni Paolo II
132, 84084 Fisciano, Salerno, Italy
Email: guida@unisa.it

ABSTRACT

In this paper, a new computational algorithm for the numerical solution of the adjoint equations for the nonlinear optimal control problem is introduced. To this end, the main features of the optimal control theory are briefly reviewed and effectively employed to derive the adjoint equations for the active control of a mechanical system forced by external excitations. A general nonlinear formulation of the cost functional is assumed and a feedforward (open-loop) control scheme is considered in the analytical structure of the control architecture. By doing so, the adjoint equations resulting from the optimal control theory enter into the formulation of a nonlinear differential-algebraic two-point boundary value problem, which mathematically describes the solution of the motion control problem under consideration. For the numerical solution of the problem at hand, an adjoint-based control optimization computational procedure is developed in this work to effectively and efficiently compute a nonlinear optimal control policy. A numerical example is provided in the paper to show the principal analytical aspects of the adjoint method. In particular, the feasibility and the effectiveness of the proposed adjoint-based numerical procedure are demonstrated for the reduction of the mechanical vibrations of a nonlinear two-degree-of-freedom dynamical system.

1 Introduction

From a general perspective, the adjoint method is a versatile mathematical tool for solving the optimal control problem in the general case of nonlinear mechanical systems [1]. The main feature of the adjoint sensitivity analysis can be described as follows: in the case of an initial value problem for a nonlinear mechanical system subjected to a prescribed control action, the sensitivity of a given objective function with respect to the controlled input parameters can be effectively computed by using a linear adjoint procedure that has approximately the same computational cost of the original dynamical simulation [2], [3], [4]. On the other hand, in the conventional linearization approach, a set of separate linearized problems needs to be independently solved for each increment of the controlled input variables in order to find an optimal control policy [5]. As a result, the application of the linearization method to optimal control problems leads to the well-known dynamic programming computational procedure [6]. The dynamic programming method suffers from the important drawback of the so-called curse of dimensionality. The curse of dimensionality is a general phenomenon in the domain of numerical analysis. In particular, for nonlinear control optimization problems, the curse of dimensionality means that the dimension and the complexity of the

problem at hand grow exponentially with respect to the number of the state and control variables [7]. Thus, the linearization procedure is considerably less general and less efficient compared to the adjoint method [8], [9]. Furthermore, another important aspect of the adjoint method is the fact that it can be successfully employed to deal with linear as well as nonlinear optimal control problems in a simple and general way [10], [11]. In the case of linear dynamical systems, several effective algorithms based on the adjoint method were developed for fluid mechanics applications in order to solve large optimal control problems bypassing the solution of the Riccati equations [12], [13]. On the other hand, only recently the adjoint method has been employed in the field of robotics and for the design, optimization, and control of mechanical systems [14], [15], [16]. Thus, the use of the adjoint analysis in the general field of applied mechanics is still at an early stage. This paper represents a step towards a further analytical and computational development of the adjoint-based analysis for controlling rigid and flexible multibody systems characterized by nonlinear differential-algebraic equations of motion [17]. To this end, a novel method to derive feedforward control actions for solving the optimal control problem of nonlinear mechanical systems is proposed in this investigation. More specifically, the general-purpose computational method developed in this work is called the adjoint-based control optimization procedure and is applied for solving the control problem of nonlinear vibrations.

The study of the nonlinear behavior of mechanical systems represents an important research topic in many fields of engineering and physics [18], [19], [20], [21], [22]. In general, a mechanical system can exhibit a linear or a nonlinear dynamical behavior [23], [24]. In particular, mechanical systems are generally influenced by different energy sources that can excite linear or nonlinear vibrations [25], [26], [27]. In many engineering applications, the problem of vibration control is of primary importance and a large amount of research has been devoted to this issue [28], [29], [30]. From a general perspective, the control strategies adopted to address this issue can be classified into two general categories, namely the active control approach and the passive control approach [31], [32]. Active control systems can be more advantageous than their passive counterparts featuring comparable performances [33], [34]. While passive control systems are relatively simple to realize, the design of an effective control policy for a nonlinear mechanical system controlled using the active approach is generally more complex, especially in the case of flexible multibody systems [35], [36], [37], [38]. In recent years, considerable research efforts have been devoted to the design of control strategies for the simultaneous suppression of structural vibrations and attenuation of contact forces in nonlinear mechanical systems [39], [40], [41]. In fact, a crucial aspect of the motion control problem for nonlinear mechanical systems is the capacity to handle the interaction between the system and the external environment [42], [43]. The adjoint method, on the other hand, can be employed as a control optimization strategy which is suitable to deal with a broad class of nonlinear dynamical problems [44], [45], [46], [47]. As shown in the paper, the adjoint-based control optimization procedure developed in this investigation can be effectively employed for solving the vibration and interaction control problem of nonlinear mechanical systems.

This paper is organized as follows. Section 2 recalls the main mathematical features of the adjoint method for nonlinear optimal control. In Section 3, the numerical implementation of the proposed adjoint-based nonlinear control optimization algorithm is discussed. Subsequently, Section 4 describes a demonstrative numerical example based on a two-degree-of-freedom nonlinear dynamical system in order to analyze the active control problem and the external isolation problem in the case of mechanical vibrations. Finally, Section 5 includes a summary and the conclusions of the paper.

2 Adjoint Method for Nonlinear Optimal Control

In this section, the basic elements of the optimal control theory and the practical implementation of the adjoint method are briefly reviewed. To this end, the necessary conditions that arise from the analytical solution of the nonlinear optimal control problem for continuous-time dynamical systems are derived considering a general case in which a feedforward control strategy is employed.

A feedforward or open-loop controller is a control policy determined as an explicit function of time and of the specific initial conditions of the dynamical system under examination [48], [49]. Consider a set of n nonlinear differential equations which describes the state evolution of a continuous-time dynamical system:

$$\begin{cases} \dot{\mathbf{z}} = \mathbf{f} \\ \mathbf{z}|_{t=0} = \mathbf{z}_0 \end{cases} \tag{1}$$

where t is time, $\mathbf{z} \equiv \mathbf{z}(t)$ denotes a n-dimensional vector representing the system state, $\mathbf{z}_0$ is a n-dimensional vector representing the system initial conditions, $\mathbf{f} \equiv \mathbf{f}(t, \mathbf{z}, \mathbf{u}, \mathbf{r})$ identifies a n-dimensional vector function that regulates the time evolution of the system state, $\mathbf{u} \equiv \mathbf{u}(t)$ is a m_u-dimensional vector of feedforward control actions and $\mathbf{r} \equiv \mathbf{r}(t)$ denotes a m_r-dimensional vector of external inputs. The vector function $\mathbf{f}$ represents a set of n nonlinear ordinary differential equations that mathematically describes the dynamics of the continuous-time system or plant to be controlled. On the other hand, one can assume a

scalar cost functional $J \equiv J(\mathbf{z}_0)$ featuring the following analytical form:

$$J = h|_{t=T} + \int_0^T g dt \tag{2}$$

where T is a fixed time domain for the control actuation, $h \equiv h(t, \mathbf{z}, \tilde{\mathbf{z}})$ is a scalar function that identifies the terminal cost function, $g \equiv g(t, \mathbf{z}, \tilde{\mathbf{z}}, \mathbf{u}, \tilde{\mathbf{u}}, \mathbf{r}, \tilde{\mathbf{F}})$ is a scalar function that denotes the current cost function, $\tilde{\mathbf{z}} \equiv \tilde{\mathbf{z}}(t)$ is a n-dimensional vector representing a preassigned reference state trajectory, $\tilde{\mathbf{u}} \equiv \tilde{\mathbf{u}}(t)$ is a m_u-dimensional vector representing a precomputed reference control action and $\tilde{\mathbf{F}} \equiv \tilde{\mathbf{F}}(t)$ is an l-dimensional vector representing an assumed reference interaction vector. Without loss of generality, the reference functions $\tilde{\mathbf{z}}$, $\tilde{\mathbf{u}}$, and $\tilde{\mathbf{F}}$ are typically set equal to zero vectors in the case of regulation problems whereas in tracking problems these functions result from the numerical solution of a previously solved motion planning problem. It is important to note that the performance index J is selected by the analyst in order to make the plant exhibit a desired type of dynamical behaviour. In fact, the cost functional J is a mathematical entity which reflects how well a specific control law $\mathbf{u}$ meets the design goals and, therefore, it is employed as a metric to quantitatively assess the performances of a dynamical system subjected to a particular set of control actions. Thus, in the case of a feedforward controller, the optimal control problem consists of finding an optimal feedforward control action $\mathbf{u}^* \equiv \mathbf{u}^*(t)$ which causes the dynamical system to follow an optimal trajectory $\mathbf{z}^* \equiv \mathbf{z}^*(t)$ that corresponds to a global minimum of the cost functional $J^* \equiv J^*(\mathbf{z}_0)$ [50], [51]. In other words, from a mathematical point of view, the problem at hand for the feedforward optimal control is to find the minimum of the cost functional (2) subjected to a set of differential constraint equations which represents analytically the system dynamical model (1). Thus, the key idea to solve this challenging mathematical problem is to consider the system dynamical model as a set of differential constraint equations for the minimization problem under consideration and, therefore, the adjoint method can be employed to define an augmented cost functional $\bar{J} \equiv \bar{J}(\mathbf{z}_0)$. To this end, the system state-space equations of motion (1) can be adjoined to the cost functional (2) in order to obtain an augmented cost functional defined as follows:

$$\bar{J} = h|_{t=T} + \int_0^T g + \boldsymbol{\lambda}^T (\mathbf{f} - \dot{\mathbf{z}}) dt \tag{3}$$

where $\boldsymbol{\lambda} \equiv \boldsymbol{\lambda}(t)$ defines a costate or adjoint state vector which identifies the Lagrange multipliers resulting from the adjoining process of the system equations of motion to the cost functional. An effective method to address the problem under study is to resort to the Pontryagin minimum principle. In order to simplify the mathematical derivation of the necessary equations which lead to the minimum of the augmented cost functional (3), a Hamiltonian function $H \equiv H(t, \mathbf{z}, \tilde{\mathbf{z}}, \mathbf{u}, \tilde{\mathbf{u}}, \mathbf{r}, \tilde{\mathbf{F}})$ can be utilized. The Hamiltonian function H is defined as:

$$H = g + \boldsymbol{\lambda}^T \mathbf{f} \tag{4}$$

According to the Pontryagin minimum principle, an optimal control action $\mathbf{u}^* \equiv \mathbf{u}^*(t)$ produces an optimal state trajectory $\mathbf{z}^* \equiv \mathbf{z}^*(t)$ that corresponds to an unconstrained minimum of the Hamiltonian function $H^* \equiv H^*(t, \mathbf{z}^*, \tilde{\mathbf{z}}, \mathbf{u}^*, \tilde{\mathbf{u}}, \mathbf{r}, \tilde{\mathbf{F}})$ [52], [53]. Hence, using the definition of the Hamiltonian function (4), the augmented cost functional (3) can be rewritten as:

$$\bar{J} = h|_{t=T} + \int_0^T H - \boldsymbol{\lambda}^T \dot{\mathbf{z}} dt \tag{5}$$

The augmented cost functional $\bar{J}$ can be reformulated by using the integration by parts rule in order to explicitly obtain the time derivative of the adjoint state $\boldsymbol{\lambda}$ as follows:

$$\bar{J} = h|_{t=T} - \boldsymbol{\lambda}^T \mathbf{z}\big|_{t=T} + \boldsymbol{\lambda}^T \mathbf{z}\big|_{t=0} + \int_0^T H + \dot{\boldsymbol{\lambda}}^T \mathbf{z} dt \tag{6}$$

By virtue of the fundamental theorem of the calculus of variation, the variation of the augmented cost functional $\bar{J}$ vanishes on an extremal state trajectory $\mathbf{z}^*$ caused by an extremal control policy $\mathbf{u}^*$ [54]. Indeed, the first variation of the augmented

cost functional $\bar{J}$ with respect to the system state $\mathbf{z}$ and with respect to the control action $\mathbf{u}$ yields:

$$\begin{aligned}\delta\bar{J} = &\left(\left(\tfrac{\partial h}{\partial \mathbf{z}}\right)^T - \lambda\right)^T \delta\mathbf{z}\Big|_{t=T} + \lambda^T \delta\mathbf{z}\big|_{t=0} + \\ &+ \int_0^T \left(\left(\tfrac{\partial H}{\partial \mathbf{z}}\right)^T + \dot{\lambda}\right)^T \delta\mathbf{z} + \tfrac{\partial H}{\partial \mathbf{u}} \delta\mathbf{u} dt\end{aligned} \tag{7}$$

The mathematical form of the variation of the augmented cost functional (7) can be considerably simplified introducing the following definitions:

$$\begin{cases} \mathbf{A} = \tfrac{\partial \mathbf{f}}{\partial \mathbf{z}}, & \mathbf{B} = \tfrac{\partial \mathbf{f}}{\partial \mathbf{u}} \\ \nu = \tfrac{\partial h}{\partial \mathbf{z}}, & \varphi = \tfrac{\partial g}{\partial \mathbf{z}}, \quad \psi = \tfrac{\partial g}{\partial \mathbf{u}} \end{cases} \tag{8}$$

where $\mathbf{A} \equiv \mathbf{A}(t, \mathbf{z}, \mathbf{u}, \mathbf{r})$ is a $n \times n$ matrix that represents the sensitivity of the system state function $\mathbf{f}$ with respect to the system state $\mathbf{z}$, $\mathbf{B} \equiv \mathbf{B}(t, \mathbf{z}, \mathbf{u}, \mathbf{r})$ denotes a $n \times m_u$ matrix representing the sensitivity of the system state function $\mathbf{f}$ with respect to the control action $\mathbf{u}$, $\nu \equiv \nu(t, \mathbf{z}, \tilde{\mathbf{z}})$ identify a n-dimensional vector that describes the sensitivity of the terminal cost function h with respect to the state vector $\mathbf{z}$, $\varphi \equiv \varphi(t, \mathbf{z}, \tilde{\mathbf{z}}, \mathbf{u}, \tilde{\mathbf{u}}, \mathbf{r}, \tilde{\mathbf{F}})$ is a n-dimensional vector describing the sensitivity of the current cost function g with respect to the system state $\mathbf{z}$ and $\psi \equiv \psi(t, \mathbf{z}, \tilde{\mathbf{z}}, \mathbf{u}, \tilde{\mathbf{u}}, \mathbf{r}, \tilde{\mathbf{F}})$ is a m_u-dimensional vector that denotes the sensitivity of the current cost function g with respect to the control vector $\mathbf{u}$. By using the definitions of the system sensitivity matrices and vectors provided by the equations (8), the variation of the augmented cost functional (7) can be rewritten as:

$$\begin{aligned}\delta\bar{J} = &\left(\nu^T - \lambda\right)^T \delta\mathbf{z}\Big|_{t=T} + \lambda^T \delta\mathbf{z}\big|_{t=0} + \\ &+ \int_0^T \left(\varphi^T + \mathbf{A}^T\lambda + \dot{\lambda}\right)^T \delta\mathbf{z} dt + \\ &+ \int_0^T \left(\psi^T + \mathbf{B}^T\lambda\right)^T \delta\mathbf{u} dt = 0\end{aligned} \tag{9}$$

Finally, assuming that the system initial state $\mathbf{z}_0$ is given and considering a fixed time horizon T, the necessary conditions which identify an optimal feedforward controller can be derived setting equal to zero the coefficients of the first variation of the augmented cost functional $\bar{J}$ with respect to the system state $\mathbf{z}$ and with respect to the control action $\mathbf{u}$ as follows:

$$\begin{cases} \dot{\mathbf{z}} = \mathbf{f}, \quad \mathbf{z}|_{t=0} = \mathbf{z}_0 \\ -\dot{\lambda} = \varphi^T + \mathbf{A}^T\lambda, \quad \lambda|_{t=T} = \nu^T\big|_{t=T} \\ \psi^T + \mathbf{B}^T\lambda = \mathbf{0} \end{cases} \tag{10}$$

The resulting differential-algebraic equations given by (10) constitute a nonlinear two-point boundary value problem and represent the necessary conditions which define the minimum of the augmented cost functional $\bar{J}$ [55], [56]. In particular, the first vector equation of the set (10) mathematically describes the direct problem, namely the dynamical evolution of the system state $\mathbf{z}$ based on the system initial conditions, whereas the second vector equation of the set (10) mathematically represents the adjoint problem, namely the dynamical evolution of the adjoint state λ based on the corresponding set of boundary or terminal conditions. On the other hand, the third vector equation of the set (10) is called the stationarity equation and defines the minimum of the Hamiltonian function H. It is important to note that the nonlinear ordinary differential equations representing the direct problem, the linear ordinary differential equations that characterize the adjoint problem, and the linear algebraic equations which identify the stationarity conditions are highly coupled and form a nonlinear differential-algebraic two-point boundary value problem. In general, these problems are challenging to solve analytically. However, there are some numerical procedures that can be effectively used to solve this type of mathematical problems. For instance, among the gradient-based optimization techniques, the iterative adjoint-based control optimization algorithm is an efficient and effective computational method capable of designing feedforward control actions for nonlinear mechanical systems [57], [58]. However, since the adjoint analysis represents a general analytical framework rather than a specific implementation procedure, in this paper the adjoint-based control optimization algorithm is developed as a numerical resolution tool in order to practically address the control problem for nonlinear mechanical systems.

3 Adjoint-Based Nonlinear Control Optimization Procedure

In this section, the numerical implementation of the adjoint-based control optimization method is discussed in detail and the complete procedure for the computer implementation of the proposed iterative technique is described step by step. In fact, the variational approach presented in the corresponding previous subsection leads to a nonlinear differential-algebraic two-point boundary value problem that, in general, cannot be solved analytically to obtain an optimal feedforward control law. Therefore, one must resort to numerical methods in order to solve such challenging nonlinear problems. To this end, there are three general classes of computational methods that can be employed to solve the problem at hand numerically, namely the neighboring extremal methods, the quasilinearization methods, and the gradient methods [59]. In particular, the numerical technique presented here belongs to the class of the gradient-based optimization methods and is able to determine an optimal feedforward control action together with the corresponding state trajectory.

The adjoint-based control optimization method represents an iterative numerical algorithm that can be effectively used to find an approximate solution to the nonlinear differential-algebraic two-point boundary value problem defined by equations (10) which identifies an optimal feedforward controller and the corresponding evolution of the system state. The main concept behind this numerical method originates from the field of computational fluid dynamics and is particularly suitable to compute in an efficient and effective way a set of feedforward control actions for mechanical systems featuring a large number of degrees of freedom. The fundamental idea of this gradient-based method is to cleverly exploit the information of the cost functional gradient, which is known analytically, in order to solve the minimization problem at hand via nonlinear optimization techniques. For this purpose, the stationarity equations are rewritten as follows for the sake of simplicity:

$$\psi^T + \mathbf{B}^T \lambda = \mathbf{0} \tag{11}$$

Indeed, for a general state trajectory corresponding to a non-optimal feedforward control action, the sationarity equations are not satisfied and, therfore, the non-zero cost functional gradient can be computed using the stationarity conditions (11) as follows:

$$\mathbf{G} = \psi^T + \mathbf{B}^T \lambda \tag{12}$$

where $\mathbf{G} \equiv \mathbf{G}(t, \mathbf{z}, \tilde{\mathbf{z}}, \mathbf{u}, \tilde{\mathbf{u}}, \mathbf{r}, \tilde{\mathbf{F}})$ is a n-dimensional vector that represents the cost functional gradient with respect to the feedforward control action for a given instant of time. For the sake of clarity, the adjoint state equations are rewritten here:

$$\begin{cases} -\dot{\lambda} = \varphi^T + \mathbf{A}^T \lambda \\ \lambda|_{t=T} = \nu^T\big|_{t=T} \end{cases} \tag{13}$$

Note that in correspondence to a non-optimal feedforward control action $\mathbf{u}$ that yields a non-extremal state trajectory $\mathbf{z}$, the cost functional gradient $\mathbf{G}$ is not a zero vector. Thus, considering a trial time history of the control action $\mathbf{u}^k$, where the superscript k refers to the index of the iterative algorithm, first the system state equations (1) must be solved numerically by using the trial time history of the feedforward control action $\mathbf{u}^k$ and then the system adjoint equations (13) must be solved numerically in order to obtain, respectively, a trial time history of the system state $\mathbf{z}^k$ and a trial time history of the adjoint state λ^k. The numerical solutions $\mathbf{z}^k$ and λ^k obtained following this procedure will satisfy, respectively, the initial conditions and the terminal conditions. Subsequently, considering a general step of the iterative adjoint-based control optimization method, the time histories $\mathbf{z}^k$ and λ^k arising from the numerical procedure will not identify the minimum of the cost functional and, therefore, the norm of the corresponding time history of the cost functional gradient $\mathbf{G}^k$ will be different from zero. The time history of the cost functional gradient $\mathbf{G}^k$ can be computed explicitly from the gradient equations (12) once the time history of the system state $\mathbf{z}^k$ and the time history of the adjoint state λ^k are known as follows:

$$\mathbf{G}^k = \left(\psi^k\right)^T + \left(\mathbf{B}^k\right)^T \lambda^k \tag{14}$$

where ψ^k and $\mathbf{B}^k$ denote respectively the time history of the cost-to-go sensitivity vector with respect to the control action and the time history of the state function sensitivity matrix with respect to the control action, both corresponding to the trial solution $\mathbf{u}^k$. The time history of the cost functional gradient $\mathbf{G}^k$ can be used in an iterative gradient-based optimization algorithm in order to gradually improve the time history of the control action $\mathbf{u}^k$ towards the minimum of the cost functional. Typically, to accomplish this task a line search algorithm is used. In general, the line search strategy leads to three general

families of minimization methods, namely the steepest descent method, the conjugate gradient methods, and the quasi-Newton methods [60]. For this purpose, all the algorithms based on the line search strategy utilize the information of the cost functional gradient $\mathbf{G}^k$ to determine a time history of the descent direction $\mathbf{e}^k$ and search the minimum of the cost functional along this direction. For instance, the steepest descent method simply sets the descent direction equal to the opposite of the cost function gradient:

$$\mathbf{e}^k = -\mathbf{G}^k \tag{15}$$

The basic idea is to perform the line search of the minimum along the direction where the cost function decreases more rapidly. However, it can be shown that this method leads to a slow convergence rate in some optimization problems because the choice of the descent direction is too rigid. On the other hand, in the nonlinear conjugate gradient method the descent direction is defined as follows:

$$\mathbf{e}^k = -\mathbf{G}^k + \beta^k \mathbf{e}^{k-1} \tag{16}$$

where $\beta^k \equiv \beta^k(\mathbf{e}^k, \mathbf{e}^{k-1})$ is a correction parameter which optimizes the direction search $\mathbf{e}^k$ and ensures that the descent directions $\mathbf{e}^k$ and $\mathbf{e}^{k-1}$ are reciprocally conjugate [61]. Furthermore, in the the quasi-Newton methods the selection of the search direction is based on an approximate estimation of the Hessian matrix computed employing the time history of the gradient vector and, as a result, a more complex calculation is involved for determining the descent direction $\mathbf{e}^k \equiv \mathbf{e}^k(\mathbf{e}^{k-1}, \mathbf{G}^k, \mathbf{G}^{k-1})$. After the selection of the search direction, a minimization procedure can be employed to optimize the time history of the control action. The minimization process starts from the current time history of the control action $\mathbf{u}^k$ and leads to the next time history of the control action $\mathbf{u}^{k+1}$ that corresponds to a lower value of the cost functional. Thus, using a line search method the time history of the control input can be iteratively updated as follows:

$$\mathbf{u}^{k+1} = \mathbf{u}^k + \alpha^k \mathbf{e}^k \tag{17}$$

where α^k is a scalar line parameter which represents the step length corresponding to the current iteration. The minimization algorithms based on a line search strategy differ from each other on the computational method employed to determine the time history of the descent direction $\mathbf{e}^k$ using the time history of the cost functional gradient $\mathbf{G}^k$. Once the time history of the descent direction $\mathbf{e}^k$ is set, the solution for the step length α^k can be found by employing a minimum search algorithm. That is:

$$\alpha^k = \underset{\alpha}{\operatorname{argmin}}\,(J) \tag{18}$$

The complete procedure necessary for the implementation of the adjoint-based control optimization method can be summarized as follows:

Step 1 - *Direct Problem Solution*: use the current time history of the feedforward control action $\mathbf{u}^k$ (or a trial feedforward control time history $\mathbf{u}^0$ for the first iteration) to integrate the system state-space equations (1) numerically forward in time starting from the set of initial conditions $\mathbf{z}|_0 = \mathbf{z}_0$ in order to obtain the current state trajectory $\mathbf{z}^k$. For instance, the explicit or implicit Runge-Kutta methods can be used to accomplish this task.
Step 2 - *Adjoint Problem Solution*: use the current state trajectory $\mathbf{z}^k$ to integrate the system adjoint state equations (13) numerically backward in time starting from the set of terminal conditions $\lambda|_T = \nu|_T$ in order to obtain the current adjoint state trajectory λ^k. The explicit or implicit Runge-Kutta methods can be used to accomplish this task as well.
Step 3 - *Gradient Computation*: use the current state trajectory $\mathbf{z}^k$ and the current adjoint state trajectory λ^k to compute the current time history of the cost functional gradient $\mathbf{G}^k$ by using its explicit expression (14) which derives from the stationary equations (11).
Step 4 - *Search Direction Computation*: use the current time history of the cost functional gradient $\mathbf{G}^k$ to compute the current time history of the search direction $\mathbf{e}^k$. For instance, the steepest descent method, the conjugate gradient methods (such as the Fletcher-Reeves algorithm, the Polak-Ribiere algorithm, or the Hestenes-Stiefel algorithm), or the quasi-Newton methods (such as the Davidon-Fletcher-Powell algorithm or the Broyden-Fletcher-Goldfarb-Shanno algorithm) can be used to accomplish this task.
Step 5 - *Initial Guess Computation*: determine an initial guess for the step length α^0 in order to initialize the minimum search algorithm. For instance, the Taylor series method can be used to accomplish this task.

Step 6 - *Bracketing*: use the initial guess for the step length α^0 to bracket the minimum of the cost functional J in an interval a^0, b^0, and c^0 along the time history of the search direction $\mathbf{e}^k$. For instance, the Fibonacci method or the golden section method can be used to accomplish this task.
Step 7 - *Minimization*: use the bracketed interval a^0, b^0, and c^0 to minimize the cost functional J along the time history of the search direction $\mathbf{e}^k$ in order to find the corresponding step length α^k and to update the time history of the control action $\mathbf{u}^{k+1}$ using the line search strategy (17). For instance, the Fibonacci search method, the golden section search method, or the Brent search method can be used to accomplish this task. If the selected convergence criteria are not satisfied, restart from step 1. For instance, a tolerance on the absolute value of the difference between the current cost functional value J^k and the past cost functional value J^{k-1} or a tolerance on the norm of current time history of the cost functional gradient $\mathbf{G}^k$ can be used to accomplish this task.

The iterative adjoint-based control optimization method leads to a numerical solution of the nonlinear differential-algebraic two-point boundary value problem defined by the equations (10) and provides the time history of the feedforward control action $\mathbf{u}^*$, the time history of the system state trajectory $\mathbf{z}^*$, and the time history of the adjoint state trajectory λ^* corresponding to a minimum of the cost functional J^*.

4 Numerical Results and Discussion

In this section, a numerical example is provided in order to describe the computer implementation of the adjoint-based control optimization procedure and demonstrate the effectiveness of the adjoint method for solving nonlinear optimal control problems. The nonlinear dynamical system analyzed in this numerical example features a simple but illustrative structure so that the sensitivity matrices necessary to implement the adjoint equations can be analytically derived.

The dynamical system considered as case-study is a lumped parameter nonlinear mechanical system featuring two degrees of freedom and is shown in figure 1. In figure 1, the first mass is denoted with m_1 and the second mass is denoted with m_2. The displacement of the first mass is represented by the coordinate $x_1 \equiv x_1(t)$ while the displacement of the second mass is represented by the coordinate $x_2 \equiv x_2(t)$. The whole system is subjected to a constant gravitational field whose gravitational acceleration is g. The mechanical system under consideration features three elastic components which exert three different force fields. The first, the second, and the third elastic components provide stiffness coefficients respectively denoted with k_1, k_2, and k_3 while the corresponding force fields feature degrees of nonlinearity that are respectively represented by the parameters η_1, η_2, and η_3. The cubic nonlinear characteristics of the first elastic components are meant to model in a simple manner the stiffening phenomenon of the system springs. Therefore, the nonlinear force fields produced by the elastic components are respectively denoted with $F_{k_1} \equiv F_{k_1}(t,x_1)$, $F_{k_2} \equiv F_{k_2}(t,x_1,x_2)$, and $F_{k_3} \equiv F_{k_3}(t,x_2)$ whereas their structures are assumed as follows:

$$\begin{cases} F_{k_1} = -k_1\Delta_1\left(1+\eta_1\Delta_1^2\right) \\ F_{k_2} = -k_2\Delta_2\left(1+\eta_2\Delta_2^2\right) \\ F_{k_3} = -k_3\Delta_3\left(1+\eta_3\Delta_3^2\right) \end{cases} \tag{19}$$

where:

$$\begin{cases} \Delta_1 = x_1 \\ \Delta_2 = x_1 - x_2 \\ \Delta_3 = x_2 - L - s \end{cases} \tag{20}$$

The first, the second, and the third dissipative components shown in figure 1 produce three linear dissipative force fields whose damping are represented respectively by the coefficients r_1, r_2, and r_3. The system is hinged on a moving support located at a height L. The displacement of the floating support is identified by the time-dependent variable $s \equiv s(t)$. For the sake of simplicity, its mathematical structure is assumed to be a superposition of two harmonic functions as follows:

$$s = S_1 \sin(2\pi f_1 t) + S_2 \sin(2\pi f_2 t) \tag{21}$$

where S_1 and S_2 denote the amplitudes of the two external displacements while f_1 and f_2 identify respectively the corresponding frequencies of the two harmonic signals. A control actuator is interposed between the two masses in order to reduce

the amplitude of the system vibrations induced by the floating support. To this end, a feedforward controller is considered for the structure of the control scheme and, therefore, the time-dependent action of the control actuator is denoted with $\mathbf{u} \equiv \mathbf{u}(t)$. A comprehensive list of all the system data is reported in table 1.

The mechanical system represented in figure 1 features $n_2 = 2$ degrees of freedom. Therefore, the system configuration can be easily identified considering a set of two generalized coordinates grouped in a vector $\mathbf{q} \equiv \mathbf{q}(t)$ and defined as:

$$\mathbf{q} = \begin{bmatrix} x_1 \\ \\ x_2 \end{bmatrix} \tag{22}$$

where x_1 and x_2 denote the displacements of the two masses as shown in figure 1. Employing the analytical techniques of the Lagrangian mechanics [62], [63], the system equations of motion can be formally written as:

$$\mathbf{M}\ddot{\mathbf{q}} = \mathbf{Q} \tag{23}$$

where $\mathbf{M} \equiv \mathbf{M}(t, \mathbf{q})$ is a $n_2 \times n_2$ matrix representing the system mass matrix and $\mathbf{Q} \equiv \mathbf{Q}(t, \mathbf{q}, \dot{\mathbf{q}}, s, \dot{s})$ is a n_2-dimensional vector denoting the vector of the external generalized forces acting on the system. For the problem on hand, the system mass matrix and the vector of the generalised external forces can be readily derived by using the D'Alemebert-Lagrange principle of virtual work [64], [65]. This well-established method leads to the following mathematical expressions:

$$\mathbf{M} = \begin{bmatrix} m_1 & 0 \\ \\ 0 & m_2 \end{bmatrix} \tag{24}$$

$$\mathbf{Q} = \begin{bmatrix} -m_1 g - k_1 x_1 \left(1 + \eta_1 x_1^2\right) + \\ -k_2 \left(x_1 - x_2\right) \left(1 + \eta_2 (x_1 - x_2)^2\right) + \\ -r_1 \dot{x}_1 - r_2 \left(\dot{x}_1 - \dot{x}_2\right) \\ \\ -m_2 g - k_2 \left(x_2 - x_1\right) \left(1 + \eta_2 (x_1 - x_2)^2\right) + \\ -k_3 \left(x_2 - L - s\right) \left(1 + \eta_3 (x_2 - L - s)^2\right) + \\ -r_2 \left(\dot{x}_2 - \dot{x}_1\right) - r_3 \left(\dot{x}_2 - \dot{s}\right) \end{bmatrix} \tag{25}$$

The system equations of motion (23) form a set of $n_2 = 2$ nonlinear second-order ordinary differential equations which requires a set of $2n_2 = 4$ initial conditions $\mathbf{q}_0$ and $\dot{\mathbf{q}}_0$. When a control action is applied on the system, the system equations of motion changes accordingly as follows:

$$\mathbf{M}\ddot{\mathbf{q}} = \mathbf{Q} + \mathbf{Q}_c \tag{26}$$

where $\mathbf{Q}_c \equiv \mathbf{Q}_c(t, \mathbf{q}, \dot{\mathbf{q}}, u)$ is a n_2-dimensional vector representing the vector of generalized forces arising from the control action. For the system under study, the control action is exerted by a force generated by an actuator acting between the two masses. Thus, in the case of a feedforward controller, the Lagrangian component of the control action $\mathbf{Q}_c$ can be expressed as follows:

$$\mathbf{Q}_c = \begin{bmatrix} -u \\ \\ u \end{bmatrix} \tag{27}$$

For the particular type and structure of control strategy considered, the controlled system results in an underactuated mechanical system because it features two degrees of freedom but there is only one control input. Underactuated systems represent a general class of dynamical systems particularly challenging to control and, therefore, this kind of mechanical systems is

often used to demonstrate the use of novel control methodologies [66], [67]. In order to convert the system equations of motion (23) from the configuration space to the state space, the system state vector $\mathbf{z}$ can be readily defined as:

$$\mathbf{z} = \begin{bmatrix} \mathbf{q} \\ \dot{\mathbf{q}} \end{bmatrix} = \begin{bmatrix} x_1 \\ x_2 \\ \dot{x}_1 \\ \dot{x}_2 \end{bmatrix} \tag{28}$$

Also, the vector of uncontrollable external actions $\mathbf{r} \equiv \mathbf{r}(t)$ can be written as follows:

$$\mathbf{r} = \begin{bmatrix} s \\ \\ \dot{s} \end{bmatrix} \tag{29}$$

where s and $\dot{s}$ denote respectively the displacement of the moving support and its time derivative. Once the state vector has been defined, the state space representation of the system dynamical model can be obtained by adding an identity relating the derivative of the configuration vector to the state vector so that the state space model can be formally written to give:

$$\dot{\mathbf{z}} = \mathbf{f} \tag{30}$$

where $\mathbf{f}$ represents the system state function. In the case of the feedforward controller considered for the problem at hand, the system state function $\mathbf{f}$ can be readily computed as:

$$\begin{aligned} \mathbf{f} &= \begin{bmatrix} \dot{\mathbf{q}} \\ \\ \mathbf{M}^{-1}\left(\mathbf{Q}+\mathbf{Q}_c\right) \end{bmatrix} = \\ &= \begin{bmatrix} \dot{x}_1 \\ \\ \dot{x}_2 \\ \\ -g - \frac{k_1}{m_1} x_1 \left(1+\eta_1 x_1^2\right) + \\ -\frac{k_2}{m_1}\left(x_1 - x_2\right)\left(1+\eta_2 (x_1-x_2)^2\right) + \\ -\frac{r_1}{m_1}\dot{x}_1 - \frac{r_2}{m_1}\left(\dot{x}_1 - \dot{x}_2\right) - \frac{u}{m_1} \\ \\ -g - \frac{k_2}{m_2}\left(x_2 - x_1\right)\left(1+\eta_2 (x_1-x_2)^2\right) + \\ -\frac{k_3}{m_2}\left(x_2 - L - s\right)\left(1+\eta_3 (x_2-L-s)^2\right) + \\ -\frac{r_2}{m_2}\left(\dot{x}_2 - \dot{x}_1\right) - \frac{r_3}{m_2}\left(\dot{x}_2 - \dot{s}\right) + \frac{u}{m_2} \end{bmatrix} \end{aligned} \tag{31}$$

On the other hand, the sensitivity matrix of the system state function with respect to the system state $\mathbf{A}$ can be derived by

computing the Jacobian matrix of the system state function $\mathbf{f}$ with respect to the system state $\mathbf{z}$ to yield:

$$\mathbf{A} = \frac{\partial \mathbf{f}}{\partial \mathbf{z}} = \\ = \begin{bmatrix} 0 & 0 & 1 & 0 \\ 0 & 0 & 0 & 1 \\ -\frac{k_1}{m_1}\left(1+3\eta_1 x_1^2\right) + \\ -\frac{k_2}{m_1}\left(1+3\eta_2 (x_1-x_2)^2\right) & \frac{k_2}{m_1}\left(1+3\eta_2 (x_1-x_2)^2\right) & -\frac{r_1+r_2}{m_1} & \frac{r_2}{m_1} \\ \frac{k_2}{m_2}\left(1+3\eta_2 (x_1-x_2)^2\right) & -\frac{k_2}{m_2}\left(1+3\eta_2 (x_1-x_2)^2\right) + \\ & -\frac{k_3}{m_2}\left(1+3\eta_3 (x_2-L-s)^2\right) & \frac{r_2}{m_2} & -\frac{r_2+r_3}{m_2} \end{bmatrix} \tag{32}$$

Furthermore, the sensitivity matrix of the system state function with respect to the vector of control actions $\mathbf{B}$ can be calculated considering the Jacobian matrix of the system state function $\mathbf{f}$ with respect to the control vector $\mathbf{u}$ as:

$$\mathbf{B} = \frac{\partial \mathbf{f}}{\partial \mathbf{u}} = \begin{bmatrix} 0 \\ 0 \\ -\frac{1}{m_1} \\ \frac{1}{m_2} \end{bmatrix} \tag{33}$$

It is worth to note that the sensitivity matrix $\mathbf{A}$ depends explicitly on the system state vector $\mathbf{z}$. Finally, the system state space model (30) constitutes a set of $n = 2n_2 = 4$ nonlinear first-order ordinary differential equations and requires the identification of the initial state $\mathbf{z}_0$ which arises from the set of $n = 2n_2 = 4$ initial conditions $\mathbf{q}_0$ and $\dot{\mathbf{q}}_0$.

The feedforward controller described here is an open-loop controller designed using the adjoint-based control optimization method. The control scheme which describes how the feedforward controller acts on the mechanical system under study is represented in figure 2. The purpose of this feedforward controller is to reduce the amplitudes of the vibrations induced by the moving support and, at the same time, to reduce more drastically the amplitude of the contact force between the second mass and the moving support representing the interaction of the mechanical system with the external environment. For the problem at hand, the contact force $\mathbf{F}$ can be expressed as follows:

$$F = -k_3 \left(L+s-x_2\right)\left(1+\eta_3 (x_2-L-s)^2\right) - r_3\left(\dot{s}-\dot{x}_2\right) \tag{34}$$

The terminal cost function h is designed assuming the following quadratic form:

$$\begin{aligned} h &= \tfrac{1}{2}(\mathbf{z}-\tilde{\mathbf{z}})^T \mathbf{Q}_T (\mathbf{z}-\tilde{\mathbf{z}}) = \\ &= \tfrac{1}{2}\left(Q_{T,1}x_1^2 + Q_{T,2}x_2^2 + Q_{T,3}\dot{x}_1^2 + Q_{T,4}\dot{x}_2^2\right) \end{aligned} \tag{35}$$

where $\mathbf{Q}_T$ is a diagonal weight matrix which characterizes the mathematical structure of the terminal cost function h. On the other hand, the cost-to-go function g is assumed quadratic as well and it is designed as:

$$\begin{aligned} g &= \tfrac{1}{2}(\mathbf{z}-\tilde{\mathbf{z}})^T \mathbf{Q}_z (\mathbf{z}-\tilde{\mathbf{z}}) + \tfrac{1}{2}(\mathbf{u}-\tilde{\mathbf{u}})^T \mathbf{Q}_u (\mathbf{u}-\tilde{\mathbf{u}}) + \tfrac{1}{2}\left(\mathbf{F}-\tilde{\mathbf{F}}\right)^T \mathbf{Q}_F \left(\mathbf{F}-\tilde{\mathbf{F}}\right) = \\ &= \tfrac{1}{2}\left(Q_{z,1}x_1^2 + Q_{z,2}x_2^2 + Q_{z,3}\dot{x}_1^2 + Q_{z,4}\dot{x}_2^2\right) + \tfrac{1}{2}Q_u u^2 + \tfrac{1}{2}Q_F F^2 = \\ &= \tfrac{1}{2}\left(Q_{z,1}x_1^2 + Q_{z,2}x_2^2 + Q_{z,3}\dot{x}_1^2 + Q_{z,4}\dot{x}_2^2\right) + \tfrac{1}{2}Q_u u^2 + \\ &\quad + \tfrac{1}{2}Q_F\left(k_3\left(L+s-x_2\right)\left(1+\eta_3 (x_2-L-s)^2\right) + r_3\left(\dot{s}-\dot{x}_2\right)\right)^2 \end{aligned} \tag{36}$$

where $\mathbf{Q}_z$, $\mathbf{Q}_u$ and $\mathbf{Q}_F$ are diagonal weight matrices which characterize the structure of the cost-to-go function g. The terminal cost sensitivity vector with respect to the system state ν can be readily derived by calculating the Jacobian matrix of the terminal cost function h with respect to the system state $\mathbf{z}$ to yield:

$$\nu = \frac{\partial h}{\partial \mathbf{z}} = (\mathbf{z} - \tilde{\mathbf{z}})^T \mathbf{Q}_T = \begin{bmatrix} Q_{T,1} x_1 \\ Q_{T,2} x_2 \\ Q_{T,3} \dot{x}_1 \\ Q_{T,1} \dot{x}_2 \end{bmatrix}^T \tag{37}$$

On the other hand, the cost-to-go sensitivity vector with respect to the system state φ can be obtained by computing the Jacobian matrix of the cost-to-go function g with respect to the system state $\mathbf{z}$ as follows:

$$\begin{aligned} \varphi = \tfrac{\partial g}{\partial \mathbf{z}} = (\mathbf{z} - \tilde{\mathbf{z}})^T \mathbf{Q}_z + \left(\mathbf{F} - \tilde{\mathbf{F}}\right)^T \mathbf{Q}_F \tfrac{\partial \mathbf{F}}{\partial \mathbf{z}} = \\ = \begin{bmatrix} Q_{z,1} x_1 \\ Q_{z,2} x_2 + Q_F F k_3 \left(1 + 3\eta_3 (x_2 - L - s)^2\right) \\ Q_{z,3} \dot{x}_1 \\ Q_{z,4} \dot{x}_2 + Q_F F r_3 \dot{x}_2 \end{bmatrix}^T \end{aligned} \tag{38}$$

The cost-to-go sensitivity vector with respect to the control action ψ can be obtained by deriving the Jacobian matrix of the cost-to-go function g with respect to the control action $\mathbf{u}$ as follows:

$$\psi = \frac{\partial g}{\partial \mathbf{u}} = (\mathbf{u} - \tilde{\mathbf{u}})^T \mathbf{Q}_u = Q_u (u - \tilde{u}) \tag{39}$$

The weight matrices which characterise the cost function are set as follows:

$$\begin{cases} \mathbf{Q}_T = diag(10, 10, 10, 10) \\ \mathbf{Q}_z = diag(10^2, 10^2, 10^2, 10^2) \\ \mathbf{Q}_u = 10^{-2} \\ \mathbf{Q}_F = 10^2 \end{cases} \tag{40}$$

For the design of the feedforward controller, the reference trajectory, the reference control action, and the reference interaction force are set as:

$$\begin{cases} \tilde{\mathbf{z}} = \mathbf{0} \\ \tilde{\mathbf{u}} = \mathbf{0} \\ \tilde{\mathbf{F}} = \mathbf{0} \end{cases} \tag{41}$$

where $\tilde{\mathbf{z}}$ denotes the reference trajectory, $\tilde{\mathbf{u}}$ denotes the reference control action, and $\tilde{\mathbf{F}}$ denotes the reference interaction force. Using the terminal cost sensitivity vector ν and the cost-to-go sensitivity vectors ϕ and ψ, the synthesis of a feedforward controller can be performed in order to numerically compute an optimal control action and the corresponding evolution

of the system state. Once the necessary system sensitivity matrices and vectors are identified, the adjoint-based control optimization method is implemented in order to derive an optimal feedforward controller following the computational steps described in the paper. To this end, the numerical solutions of the direct problem and of the adjoint problem, which represent steps 1 and 2 of the adjoint-based procedure, are obtained by means of the classical explicit fourth-order Runge-Kutta method considering a time step of 10^{-3} seconds and a time span of 10 seconds. The gradient-based optimization, which represents steps 3 and 4 of the adjoint-based optimization method, is performed using a quasi-Newton method based on the Broyden-Fletcher-Goldfarb-Shanno iterative algorithm. The computation of the initial guess for the minimization procedure, that represents the step 5 of the complete algorithm, is realized employing a Taylor series expansion. The bracketing and the minimization for the research of the cost functional minimum, which represent steps 6 and 7 of the proposed computational procedure, are both carried out through the implementation of the Fibonacci search technique featuring a tolerance of 10^{-9} on the relative difference of the cost functional and a tolerance of 10^{-3} for the norm of the cost functional gradient. The numerical integration necessary to evaluate the cost functional corresponding to a given set of control actions is performed using the Simpson method featuring the $3/8$-rule. The resulting iterative convergence of the relative cost functional computed with respect to the minimum reached by the numerical algorithm as $J_r^k = (J^k - J^*)/J^*$ is shown in figure 3, where the corresponding minimum value of the cost function obtained by the numerical optimization procedure is $J^* = 6.276 \cdot 10^8$. This figure shows that, in this numerical example related to the design of a feedforward control action, the adjoint-based control optimization method features a rapid convergence. However, the number of iterations necessary to achieve convergence for a preassigned set of tolerances is strongly problem-dependent. In general, the main factors that influence the convergence rate of an optimization algorithm are the initial guess and the problem parameters that define the local shape of the objective function. This issue is particularly important in the case of a dynamical optimization problem in which the resulting geometrical shape of the hypersurface associated with the performance index depends on the dynamical behavior of the system analyzed and, consequently, on the parameters that characterize the nature of the mechanical system and its initial state [68]. One simple method to address this issue is to run the adjoint-based numerical optimization procedure using multiple starting configurations and compare the numerical value of the minima obtained. This simple method was adopted for obtaining the numerical results presented in the paper. The optimal feedforward control action resulting from the adjoint-based control optimization method is depicted in figure 4. In figures 5 and 6, the dashed lines represent, respectively, the displacements of the first and second mass when the system is uncontrolled whereas the solid lines represent, respectively, the displacements of the first and second mass when the feedforward controller acts on the system. In figures 7 and 8, the dashed lines represent, respectively, the velocities of the first and second mass when the system is uncontrolled while the solid lines represent, respectively, the velocities of the first and second mass when the feedforward controller acts on the system. Qualitatively, these figures show that the effect of the feedforward control action is a considerable amplitude reduction of the system vibrations. In figure 9, the dashed line represents the interaction force when the system is uncontrolled whereas the solid line represents the interaction force when the feedforward controller acts on the system. Qualitatively, it is apparent that the action of the feedforward controller yields a sensible amplitude reduction of the system interaction force. Furthermore, the amplitude reductions of the system displacements, velocities, and interaction force can be assessed quantitatively by comparing the standard deviation values of the system response with and without the feedforward controller as shown in table 2. In this table, $\lambda_{x_1,u}$, $\lambda_{x_2,u}$, $\lambda_{\dot{x}_1,u}$, $\lambda_{\dot{x}_2,u}$, and $\lambda_{F,u}$ denote, respectively, the standard deviation values of the system displacements, velocities, and interaction force when there is no control action whereas $\lambda_{x_1,c}$, $\lambda_{x_2,c}$, $\lambda_{\dot{x}_1,c}$, $\lambda_{\dot{x}_2,c}$, and $\lambda_{F,c}$ denote, respectively, the standard deviation values of the system displacements, velocities, and interaction force when the feedforward controller acts on the system. The numerical results presented in this illustrative example demonstrate that the feedforward control action designed by using the proposed adjoint-based computational procedure has a good performance in general and show the effectiveness of the proposed methodology.

5 Summary and Conclusions

The main research goal of the authors is to develop new, effective and efficient methods to perform accurate analytic modeling [69], [70], [71], [72], [73], experimental parameter identification [74], [75], and numerical control optimization [76], [77], [78] of rigid as well as flexible mechanical systems exploiting the deep connections between multibody dynamics, system identification, and control theory.

In this investigation, the analytical derivation and the computer implementation of the adjoint method for optimal control of nonlinear mechanical systems were analyzed. To this end, the optimal control problem for nonlinear dynamical systems was addressed and numerically solved employing an iterative adjoint-based control optimization method. In particular, the numerical procedure proposed in the paper was designed in order to implement the active control paradigm for the suppression of the structural vibrations of an archetypical nonlinear dynamical system and, simultaneously, for the attenuation of the contact forces which result from the interaction of the mechanical system under consideration with the external environment. By means of numerical simulations, the synthesis of an optimal feedforward controller was obtained together with the corresponding time histories of the system state. Numerical experiments show a considerable attenuation of the amplitude of the mechanical vibrations and of the magnitude of the interaction forces, thereby demonstrating the effectiveness of the

adjoint-based computational procedure proposed in this investigation.

References

[1] Bryson, A. E., and Ho, Y. C., 1975, Applied Optimal Control - Optimization, Estimation, and Control, Taylor and Francis, New York.

[2] Luchini, P., and Bottaro, A., 2014, "An Introduction to Adjoint Problems", Annual Review of Fluid Mechanics, Supplemental Appendix A.

[3] Luchini, P., and Bottaro, A., 2014, "Adjoint Equations in Stability Analysis", Annual Review of Fluid Mechanics, 46, pp. 1-30.

[4] Bewley, T. R., 2015, Numerical Renaissance - Simulation, Optimization and Control, Renaissance Press, To be published.

[5] Bertsekas, D. P., 2005, Dynamic Programming and Optimal Control - Volume I, Athena Scientific, Belmont.

[6] Bertsekas, D. P., 2005, Dynamic Programming and Optimal Control - Volume II, Athena Scientific, Belmont.

[7] Bellman, R. E., and Dreyfus, S. E., 1962, Applied Dynamic Programming, Oxford University Press, London.

[8] Bewley, T. R., 2001, "Flow Control - New Challenges for a New Renaissance", Progress in Aerospace Sciences, 37, pp. 21-58.

[9] Kim, J., and Bewley, T. R., 2007, "A Linear Systems Approach to Flow Control", Annual Review of Fluid Mechanics, 39, pp. 383-417.

[10] Giles, M. B., and Pierce, N. A., 2000, "An Introduction to the Adjoint Approach to Design", Journal of Flow, Turbulence, and Combustion, 65, pp. 393-415.

[11] Giannetti, F., and Luchini, P., 2006, "Leading-Edge Receptivity by Adjoint Methods", Journal of Fluid Mechanics, 547, pp. 21-53.

[12] Giannetti, F., Camarri, S., and Luchini, P., 2010, "Structural Sensitivity of the Secondary Instability in the Wake of a Circular Cylinder", Journal of Fluid Mechanics, 651, pp. 319-337.

[13] Luchini, P., and Bewley, T. R., 2010, "Methods for the Solution of Very Large Flow-Control Problems that Bypass Open-Loop Model Reduction", Bulletin of the American Physical Society, 55-16, pp. 42-42.

[14] Schmidt-Wetekam, C., Zhang, D., Hughes, R., and Bewley, T. R., 2007, "Design, Optimization, and Control of a New Class of Reconfigurable Hopping Rovers", Proceedings of the 46th IEEE Conference on Decision and Control New Orleans, LA, USA, December 12-14.

[15] Summers, S., and Bewley, T. R., 2007, "MPDopt - A Versatile Toolbox for Adjoint-Based Model Predictive Control of Smooth and Switched Nonlinear Dynamic Systems", Proceedings of the 46th IEEE Conference on Decision and Control New Orleans, LA, USA, December 12-14.

[16] Bewley, T. R., Temam, R., and Zianed, M., 2000, "A General Framework for Robust Control in Fluid Mechanics", Physica D: Nonlinear Phenomena, 138(3-4), pp. 360-392.

[17] Mariti, L., Belfiore, N. P., Pennestri, E., and Valentini, P. P., 2011, "Comparison of Solution Strategies for Multibody Dynamics Equations", International Journal for Numerical Methods in Engineering, 88(7), pp. 637-656.

[18] Nayfeh, A. H., and Mook, D. T., 1995, Nonlinear Oscillations, Wiley, New York.

[19] Antman, S. S., 2005, Nonlinear Problems of Elasticity (Second Edition), Springer, New York.

[20] Meirovitch, L., 2010, Fundamentals of Vibrations, McGraw Hill, Boston.

[21] Ashour, O. N., and Nayfeh, A. H., 2002, "Adaptive Control of Flexible Structures Using a Nonlinear Vibration Absorber", Journal of Nonlinear Dynamics, 28, pp. 309-322.

[22] Siciliano, B., Sciavicco, L., Villani, L., and Oriolo, G., 2010, Robotics - Modeling, Planning and Control, Springer, London.

[23] Khalil, H. K., 2001, Nonlinear Systems (Third Edition), Prentice Hall, Upper Saddle River.

[24] Hagedorn, P., and DasGupta, A., 2007, Vibrations and Waves in Continuous Mechanical Systems, Wiley, Chichester.

[25] Preumont, A., 2011, Vibration Control of Active Structures - An Introduction (Third Edition), Springer, Berlin.

[26] Bauchau, O. A., and Craig, J. I., 2009, Structural Analysis - With Applications to Aerospace Structures, Springer, New York.

[27] Hodges, D. H., and Pierce, G. A., 2002, Introduction to Structural Dynamics and Aeroelasticity, Cambridge University Press, Cambridge.

[28] Genta, G., 2009, Vibration Dynamics and Control, Springer, New York.

[29] Inman, D. J., 2006, Vibration with Control, Wiley, Chichester.

[30] Slotine, J. E., and Li, W., 1991, Applied Nonlinear Control, Prentice Hall, Englewood Cliffs.

[31] Cheli, F., and Diana, G., 2015, Advanced Dynamics of Mechanical Systems, Springer, London.

[32] Gawronski, W. K., 2004, Advanced Structural Dynamics and Active Control of Structures, Springer, New York.

[33] Skelton, R. E., and de Oliveira, M. C., 2009, Tensegrity Systems, Springer, New York.

[34] Juang, J. N., and Phan, M. Q., 2004, Identification and Control of Mechanical Systems, Cambridge University Press, Cambridge.
[35] Seifried, R., 2014, Dynamics of Underactuated Multibody Systems - Modeling, Control, and Optimal Design, Springer, London.
[36] Zhong, W. X., 2004, Duality System in Applied Mechanics and Optimal Control, Kluwer Academic Publishers, New York.
[37] Inman, D. J., 2008, Engineering Vibration (Third Edition), Prentice Hall, Upper Saddle River.
[38] Al Majid, A., and Dufour, R., 2002, "Formulation of a Hysteretic Restoring Force Model - Application to Vibration Isolation", Journal of Nonlinear Dynamics, 27, pp. 69-85.
[39] Udwadia, F. E., 2013, "A New Approach to Stable Optimal Control of Complex Nonlinear Dynamical Systems", Journal of Applied Mechanics, 81(3), pp. 1-6.
[40] Raibert, M. H., and Craig, J. J., 1981, "Hybrid Position-Force Control of Manipulators", Journal of Dynamic Systems, Measurement, and Control, 103(2), 126-133.
[41] Gorinevsky, D., Formalsky, A., and Schneider, A., 1997, Force Control of Robotics Systems, CRC Press, Boca Raton.
[42] Spong, M. W., Hutchinson, S., and Vidyasagar, M., 2005, Robot Modeling and Control, Wiley, New York.
[43] Lewis, F. L., Dawson, D. M., and Abdallah, C. T. , 2003, Robot Manipulator Control - Theory and Practice, CRC Press, Boca Raton.
[44] Guida, D., and Pappalardo, C. M., 2015, "Control Design of an Active Suspension System for a Quarter-Car Model with Hysteresis", Journal of Vibration Engineering and Technologies, 3(3), pp. 277-299.
[45] Pappalardo, C. M., 2015, "A Natural Absolute Coordinate Formulation for the Kinematic and Dynamic Analysis of Rigid Multibody Systems", Journal of Nonlinear Dynamics, 81(4), pp. 1841-1869.
[46] Pappalardo, C. M., Patel, M. D., Tinsley, B., and Shabana, A. A., 2015, "Contact Force Control in Multibody Pantograph/Catenary Systems", Proceedings of the Institution of Mechanical Engineers, Part K: Journal of Multibody Dynamics, 0(0), pp. 1-22.
[47] Pappalardo, C. M., Yu, Z., Zhang, X., and Shabana, A. A., 2015, "Rational ANCF Thin Plate Finite Element", Journal of Computational and Nonlinear Dynamics, 11(5), pp. 1-15.
[48] Ogata, K., 2010, Modern Control Engineering (Fifth Edition), Prentice Hall, Boston.
[49] Nise, N. S., 2011, Control System Engineering (Sixth Edition), Wiley, New York.
[50] Vincent, T. L., and Grantham, J. W., 1997, Nonlinear and Optimal Control Systems, Wiley, New York.
[51] Troutman, J. L., 1995, Variational Calculus and Optimal Control - Optimization with Elementary Convexity (Second Edition), Springer, New York.
[52] Betts, J. T., 2010, Practical Methods for Optimal Control and Estimation Using Nonlinear Programming (Second Edition), Siam, Philadelphia.
[53] Liberzon, D., 2012, Calculus of Variations and Optimal Control Theory - A Concise Introduction, Princeton University Press, Princeton.
[54] Clarke, F., 2013, Functional Analysis, Calculus of Variation and Optimal Control, Springer, London.
[55] Stengel, R. F., 1986, Optimal Control and Estimation, Dover, New York.
[56] Lewis, F. L., Vrabie, D. L., and Syrmos, V. L., 2012, Optimal Control (Third Edition), Wiley, New York.
[57] Bement, M. T., and Bewley, T. R., 2008, "Excitation Design for Damage Detection using Iterative Adjoint-Based Optimization - Part 1: Method Development", Mechanical Systems and Signal Processing, 23, pp. 783-793.
[58] Bement, M. T., and Bewley, T. R., 2008, "Excitation Design for Damage Detection using Iterative Adjoint-Based Optimization - Part 2: Experimental Demonstration", Mechanical Systems and Signal Processing, 23, pp. 794-803.
[59] Kirk, D. E., 1970, Optimal Control Theory - An Introduction, Dover, Mineola.
[60] Press, W. H., Teukolsky, S. A., Vetterling, W. T., and Flannery B. P., 2007, Numerical Recipes - The Art of Scientific Computing (Third Edition), Cambridge University Press, Cambridge.
[61] Snyman, J. A., 2005, Practical Mathematical Optimization - An Introduction to Basic Optimization Theory and Classical and New Gradient-Based Algorithms, Springer, New York.
[62] Shabana, A. A., 2013, Dynamics of Multibody Systems (Forth Edition), Cambridge University Press, Cambridge.
[63] Meirovitch, L., 2010, Methods of Analytical Dynamics, Dover, Mineola.
[64] Lanczos, C., 1986, The Variational Principles of Mechanics (Fourth Edition), Dover, Mineola.
[65] Goldstein, H., Poole C. P., and Safko, J. L., 2013, Classical Mechanics (Third Edition), Addison Wesley, San Francisco.
[66] Fantoni, I., and Lozano, R., 2001, Non-linear Control for Underactuated Mechanical Systems, Springer, London.
[67] Guida, D., and Pappalardo, C. M., 2014, "Forward and Inverse Dynamics of Nonholonomic Mechanical Systems", Meccanica, 49(7), pp. 1547-1559.
[68] Nocedal, J., and Wright, S., 2006, Numerical Optimization (Second Edition), Springer, New York.
[69] Pappalardo, C. M., and Guida, D., 2016, "Control of Nonlinear Vibrations using the Adjoint Method", Meccanica, Submitted.
[70] Kulkarni, S., Pappalardo, C. M., and Shabana, A. A., 2016, "Pantograph/Catenary Contact Formulations", ASME

Journal of Vibrations and Acoustics, 139(1), pp. 1-12.
[71] Pappalardo, C. M., Wallin, M., and Shabana, A. A., 2016, "A New ANCF/CRBF Fully Parametrized Plate Finite Element", ASME Journal of Computational and Nonlinear Dynamics, 12(3). pp. 1-13.
[72] Pappalardo, C. M., Wang, T., and Shabana, A. A., 2016, "On the Formulation of the Planar ANCF Triangular Finite Elements", Journal of Nonlinear Dynamics, Submitted.
[73] Pappalardo, C. M., Wang, T., and Shabana, A. A., 2016, "New ANCF Tetrahedral Finite Elements for the Nonlinear Dynamics of Flexible Structures", Journal of Nonlinear Dynamics, Submitted.
[74] Guida, D., and Pappalardo, C. M., 2009, "Sommerfeld and Mass Parameter Identification of Lubricated Journal Bearing", WSEAS Transactions on Applied and Theoretical Mechanics, 4(4), pp. 205-214.
[75] Guida, D., Nilvetti, F., and Pappalardo, C. M., 2009, "Parameter Identification of a Two Degrees of Freedom Mechanical System", International Journal of Mechanics, 3(2), pp. 23-30.
[76] Guida, D., Nilvetti, F., and Pappalardo, C. M., 2009, "Instability Induced by Dry Friction", International Journal of Mechanics, 3(3), pp. 44-51.
[77] Guida, D., Nilvetti, F., and Pappalardo, C. M., 2009, "Dry Friction Influence on Cart Pendulum Dynamics", International Journal of Mechanics, 3(2), pp. 31-38.
[78] Guida, D., and Pappalardo, C. M., 2013, "A New Control Algorithm for Active Suspension Systems Featuring Hysteresis", FME Transactions, 41(4), pp. 285-290.

Table Captions

- Table 1. Mechanical System Data
- Table 2. Control System Performance

Figure Captions

- Figure 1. Two Degrees of Freedom Nonlinear Mechanical System
- Figure 2. Control Scheme for the Feedforward Controller
- Figure 3. Cost Function Convergence - J_r
- Figure 4. Control input - u
- Figure 5. Uncontrolled and Controlled Displacement - x_1
- Figure 6. Uncontrolled and Controlled Displacement - x_2
- Figure 7. Uncontrolled and Controlled Velocity - $\dot{x}_1$
- Figure 8. Uncontrolled and Controlled Velocity - $\dot{x}_2$
- Figure 9. Uncontrolled and Controlled Force - F

DESCRIPTIONS	SYMBOLS	DATA [UNITS]
First Mass	m_1	$3\ [\mathrm{kg}]$
Second Mass	m_2	$4\ [\mathrm{kg}]$
First Stiffness	k_1	$50\ \left[\mathrm{kg}\cdot\mathrm{s}^{-2}\right]$
Second Stiffness	k_2	$150\ \left[\mathrm{kg}\cdot\mathrm{s}^{-2}\right]$
Third Stiffness	k_3	$75\ \left[\mathrm{kg}\cdot\mathrm{s}^{-2}\right]$
First Stiffness Degree of Nonlinearity	η_1	$7\ \left[\mathrm{m}^{-2}\right]$
Second Stiffness Degree of Nonlinearity	η_2	$11\ \left[\mathrm{m}^{-2}\right]$
Third Stiffness Degree of Nonlinearity	η_3	$9\ \left[\mathrm{m}^{-2}\right]$
First Damping	r_1	$2\ \left[\mathrm{kg}\cdot\mathrm{s}^{-1}\right]$
Second Damping	r_2	$3\ \left[\mathrm{kg}\cdot\mathrm{s}^{-1}\right]$
Third Damping	r_3	$4\ \left[\mathrm{kg}\cdot\mathrm{s}^{-1}\right]$
Gravity Acceleration	g	$9.81\ \left[\mathrm{m}\cdot\mathrm{s}^{-2}\right]$
Support Height	L	$2\ [\mathrm{m}]$
Support Displacement - Amplitude 1	S_1	$0.4\ [\mathrm{m}]$
Support Displacement - Amplitude 2	S_2	$0.07\ [\mathrm{m}]$
Support Displacement - Frequency 1	f_1	$3\ \left[\mathrm{s}^{-1}\right]$
Support Displacement - Frequency 2	f_2	$15\ \left[\mathrm{s}^{-1}\right]$
Initial Displacement of First Mass	$x_{1,0}$	$0.01\ [\mathrm{m}]$
Initial Displacement of Second Mass	$x_{2,0}$	$0.02\ [\mathrm{m}]$
Initial Velocity of First Mass	$v_{1,0}$	$0.1\ \left[\mathrm{m}\cdot\mathrm{s}^{-1}\right]$
Initial Velocity of Second Mass	$v_{2,0}$	$0.2\ \left[\mathrm{m}\cdot\mathrm{s}^{-1}\right]$

Table 1. Mechanical System Data

DESCRIPTIONS	SYMBOLS	DATA [UNITS]
Displacement Amplitude Reduction of the First Mass	$\lambda_{x_1} = \frac{\lambda_{x_1,u} - \lambda_{x_1,c}}{\lambda_{x_1,u}}$	$53.554\,[\%]$
Displacement Amplitude Reduction of the Second Mass	$\lambda_{x_2} = \frac{\lambda_{x_2,u} - \lambda_{x_2,c}}{\lambda_{x_2,u}}$	$52.227\,[\%]$
Velocity Amplitude Reduction of the First Mass	$\lambda_{\dot{x}_1} = \frac{\lambda_{\dot{x}_1,u} - \lambda_{\dot{x}_1,c}}{\lambda_{\dot{x}_1,u}}$	$35.374\,[\%]$
Velocity Amplitude Reduction of the Second Mass	$\lambda_{\dot{x}_2} = \frac{\lambda_{\dot{x}_2,u} - \lambda_{\dot{x}_2,c}}{\lambda_{\dot{x}_2,u}}$	$41.237\,[\%]$
Amplitude Reduction of the Interaction Force	$\lambda_F = \frac{\lambda_{F,u} - \lambda_{F,c}}{\lambda_{F,u}}$	$46.875\,[\%]$

Table 2. Control System Performance

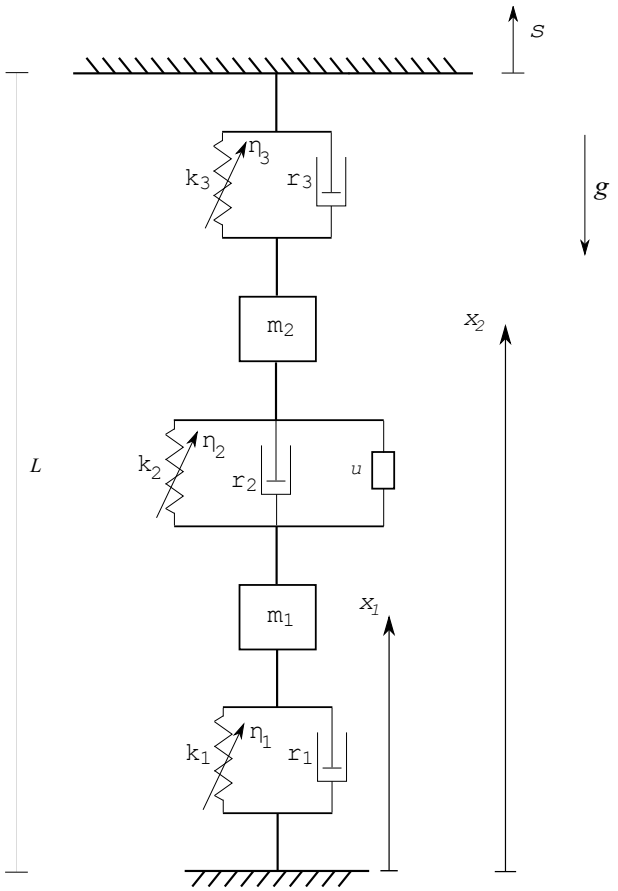

Fig. 1. Two Degrees of Freedom Nonlinear Mechanical System

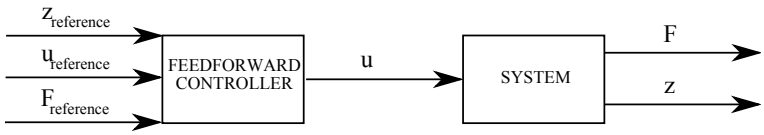

Fig. 2. Control Scheme for the Feedforward Controller

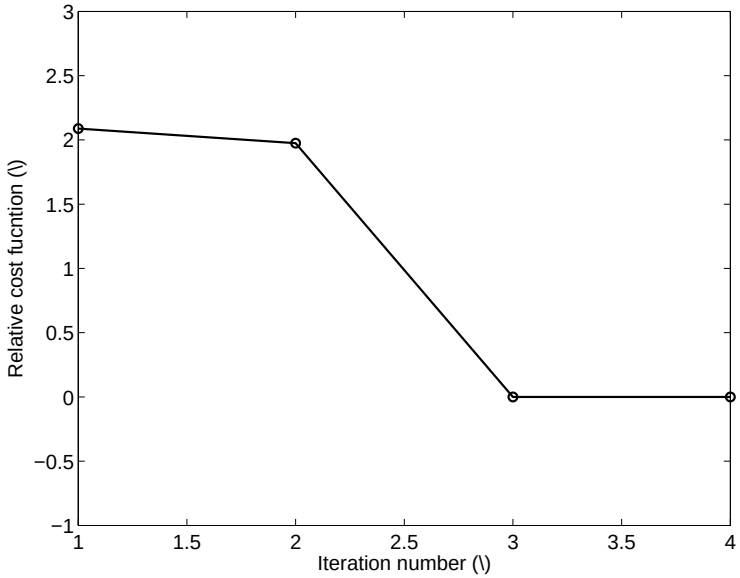

Fig. 3. Cost Function Convergence - J_r

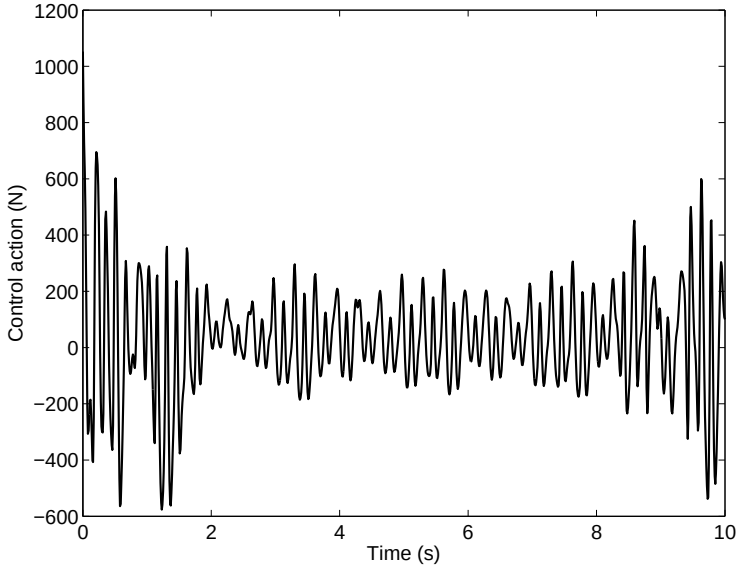

Fig. 4. Control input - u

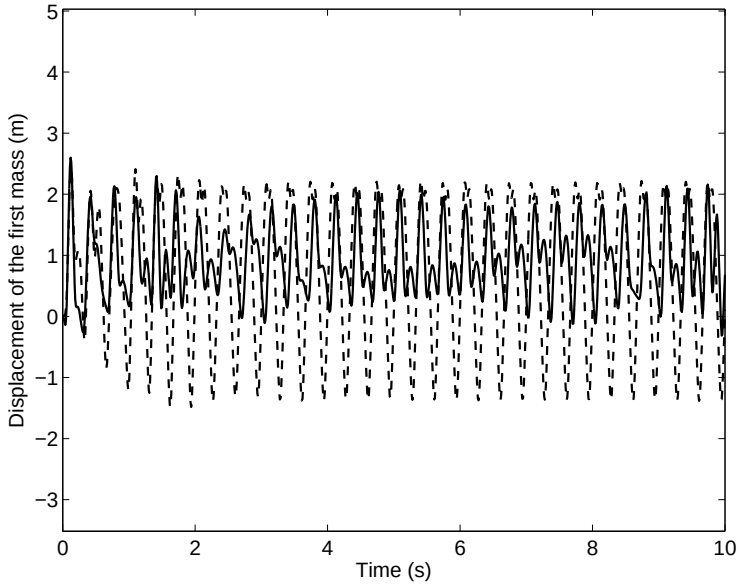

Fig. 5. Uncontrolled and Controlled Displacement - x_1

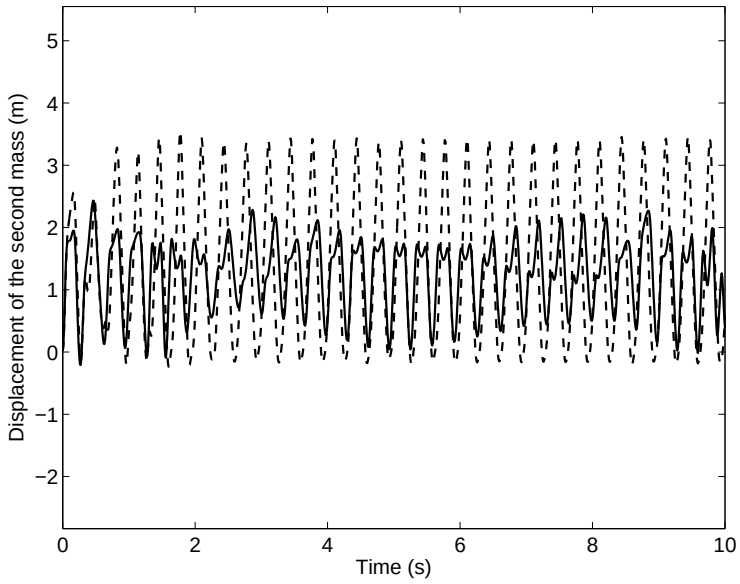

Fig. 6. Uncontrolled and Controlled Displacement - x_2

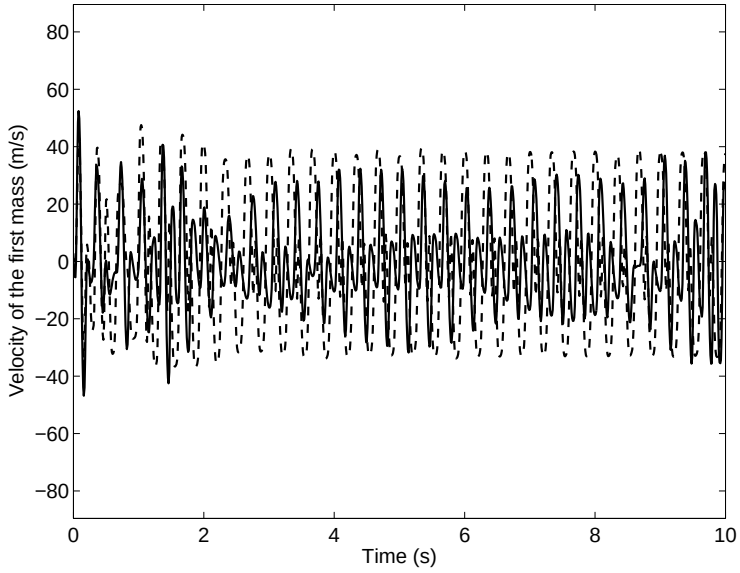

Fig. 7. Uncontrolled and Controlled Velocity - $\dot{x}_1$

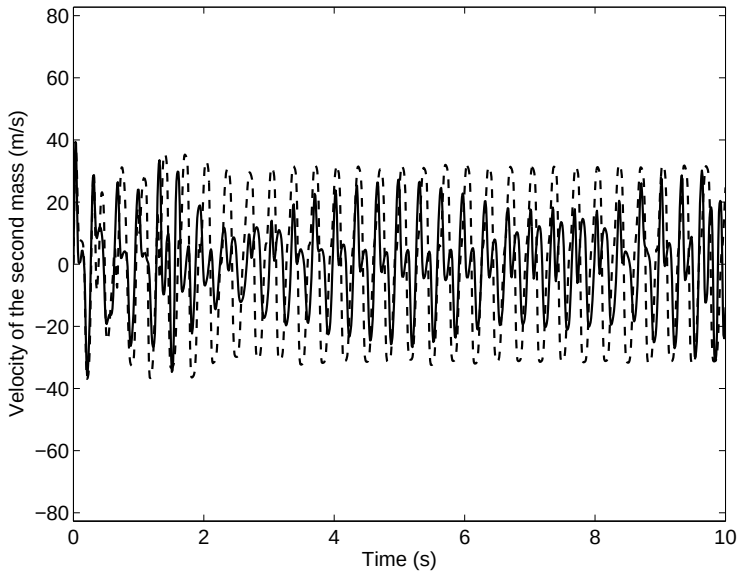

Fig. 8. Uncontrolled and Controlled Velocity - $\dot{x}_2$

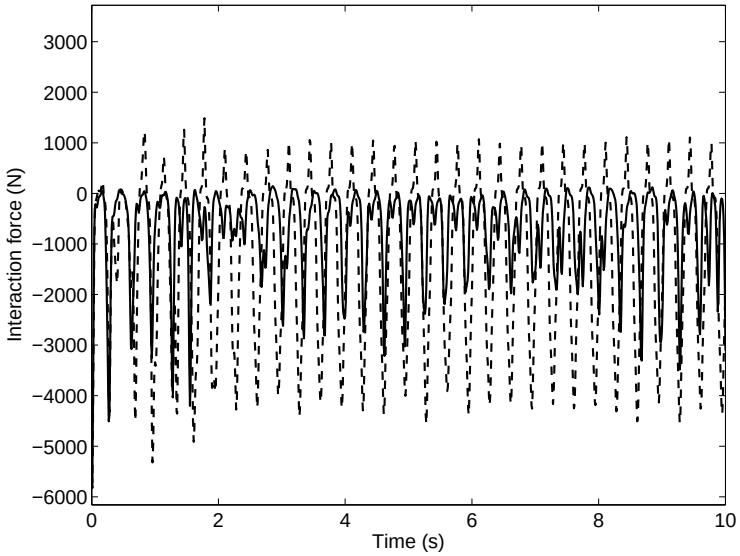

Fig. 9. Uncontrolled and Controlled Force - F